Cooperative nitrogen insertion processes: Thermal transformation of NH_3 on a Si(100) surface

J. C. F. Rodríguez-Reyes and A. V. Teplyakov*
Department of Chemistry and Biochemistry, University of Delaware, Newark, Delaware 19716, USA
(Received 10 April 2007; revised manuscript received 18 July 2007; published 30 August 2007)

The thermal behavior of an ammonia-covered Si(100) surface is investigated by infrared spectroscopy and density functional methods. Upon adsorption at room temperature, $(Si)NH_2$ and Si-H species are formed on the surface. Comparison of the vibrational studies with density functional calculations suggests that the $(Si)NH_2$ structures are preferentially located on the same side along the silicon dimer row on a (2×1) reconstructed Si(100) surface, although a mixture of different long-range configurations is likely formed. Decomposition of these $(Si)NH_2$ species is observed to start at temperatures as low as 500 K. Theoretical predictions of the vibrational modes indicate that at this point, the spectrum is composed of a combination of $(Si)_2NH$ and $(Si)_3N$ vibrational signatures, which result from insertion of N into Si-Si bonds. Our computational study of the formation of $(Si)_2NH$ structures indicates that subsurface insertion is more feasible if the strain imposed during the insertion in a Si dimer is attenuated by a $(Si)_2NH$ structure already inserted in the neighboring dimer along the same silicon dimer row. This cooperative reaction lowers the energetic requirements for subsurface insertion, providing a theoretical explanation for the mechanism of thermal decomposition of NH_3 on Si(100) and for other systems where subsurface migration is observed experimentally.

DOI: 10.1103/PhysRevB.76.075348 PACS number(s): 68.35.Ja, 68.43.Fg, 68.43.Hn

I. INTRODUCTION

Due to the importance of silicon nitride films in the semiconductor industry, the reaction of ammonia (NH_3) with the Si(100) surface has been investigated extensively. However, in spite of its apparent simplicity, the NH_3/Si(100) system has challenged many researchers for the past 20 years. Early studies observed that ammonia adsorbs dissociatively on Si(100) even at cryogenic temperatures,[1–6] and after some controversy regarding the nature of the dissociation products, it was established that NH_3 dissociates on this surface to form $(Si)NH_2$ and Si-H,[7–30] which was confirmed by theoretical studies.[31–34] Dissociation was found to be possible even at low temperatures because of the high reactivity of the Si(100) surface.[35] This surface can be best described as formed by rows of surface dimers, which result from the (2×1) reconstruction. Each dimer is buckled, forming a zwitterionic entity where the "down" atom has more of an electrophilic character, while the "up" atom can be thought of as nucleophilic. The low energy required for the buckling causes the dimers to often show up as symmetric entities at room temperature scanning tunneling microscopy (STM) studies; however, cryogenic temperature investigations indeed suggest the buckled structure.[44] Thus, the adsorption of NH_3 on this surface can be viewed as a nucleophilic attack of the N lone pair onto a down Si atom, a process that was found to be barrierless.[31–34,36] This initial process forms a tetracoordinated nitrogen atom (N_{4C}) and further stabilization of this structure is achieved by dissociation, through the cleavage of a N-H bond and the formation of the stable species $(Si)NH_2$ and Si-H.[37,38] Since the nucleophilic up atom of the silicon dimer containing the adsorbed molecule can facilitate the cleavage of the N-H bond, the intradimer dissociation was widely assumed,[31–34,36] although recent investigations, both theoretical[41–43] and experimental,[29,30] suggest that interdimer dissociation might be a significant pathway as well. Nevertheless, since the intradimer dissociation was widely accepted, other researchers studied the long-range configuration of adsorbed species, finding two possible configurations: (1) where NH_2 groups are located on the same side of the silicon dimer row (which we will refer to as *aligned*) and (2) where NH_2 groups alternate with H species along the same side of a silicon dimer row (which we will refer to as *alternate*). Optimized geometries for these configurations using a cluster representing three silicon surface dimers are shown in Fig. 1, and computational considerations regarding these geometries are fully discussed below. Although initially it was proposed that the alternate configuration is preferred,[24,25,30,40] the presence of an aligned configuration is supported by theoretical considerations,[28,45,46] and it has been observed with STM.[28]

The process of thermal decomposition of the ammonia-covered surface has also been debated intensively.[1–3,6–15,26,27,47–51] There was originally a controversy about the nature of the decomposed species formed

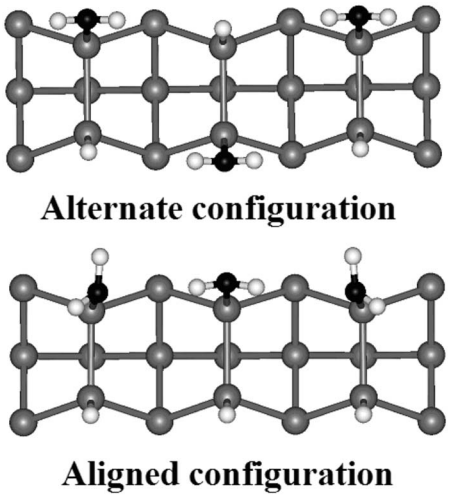

FIG. 1. Possible long-range configurations formed on the Si(100) upon dissociative adsorption of NH_3. The dimer unit consists of $(Si)NH_2$ and Si-H species. Black, nitrogen; gray, silicon; white: hydrogen.

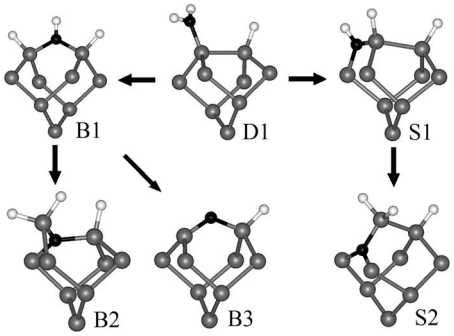

FIG. 2. Proposed pathways for decomposition of dissociatively adsorbed species. D1→B1→B2 (B3) represents the surface insertion pathway. D1→S1→S2 represents the subsurface insertion pathway. Black, nitrogen; gray, silicon; white, hydrogen.

from $(Si)NH_2$ structures as the surface is annealed. At present, it is known that there are three processes occurring during the thermal annealing of the NH_3-saturated Si(100) surface: (i) decomposition of $(Si)NH_2$ to $(Si)_2NH$ and $(Si)_3N$, which also leads to the formation of additional Si-H species;[3,6–8,10–13,26,27] (ii) desorption of ammonia and of hydrogen that have been observed to occur at 650 and 780 K, respectively;[7,9,13–15,23,47] and (iii) migration of N atoms, initially into the bulk of the Si lattice,[1,2,7,8,26,27,52] followed by their segregation back to the surface around 1000 K.[27] Widjaja and Musgrave considered two decomposition pathways, outlined in Fig. 2, and offered a detailed mechanistic picture of the possible decomposition processes.[48] In both cases, the mechanism of decomposition follows the pattern observed for dissociative adsorption: A nucleophilic attack of the N lone pair onto a Si atom and the formation of a N_{4C} structure, followed by the dissociation through scission of a N-H bond that allows the nitrogen atom to regain its tricoordination. The lone pair in $(Si)NH_2$ can attack either the surface silicon atom in the same dimer or a silicon atom in the second layer. While the first case leads to the formation of the bridged structure B1 in Fig. 2, the second case results in the formation of the backbonded structure S1. These possibilities will be hereafter referred to as *surface insertion* and *subsurface insertion*, respectively. The computational work of Widjaja and Musgrave suggested that the decomposition of $(Si)NH_2$ species is not favored kinetically unless hydrogen atoms are removed from the surface.[48] Following that suggestion, a recent computational study has been successful in explaining the segregation of N atoms from the bulk to the surface at high temperatures using a model where the hydrogen atoms have been removed from the surface.[51] These computational investigations are particularly important for the process of formation of silicon nitride films, which may involve temperatures as high as 1000 K,[53] where no H is remaining on the surface. However, if these predictions are applied to the thermal decomposition of a surface saturated with ammonia at lower temperatures, they would suggest that desorption processes have to take place in order to start the decomposition of $(Si)NH_2$ and the migration of N atoms. Since desorption processes start at 650 K,[7,9,13–15,23,47] these computational studies propose that $(Si)NH_2$ species are mostly stable up to this temperature and that later the majority of these species recombines with hydrogen and desorbs as ammonia.[48] Interestingly, temperature-programed desorption (TPD) experiments have shown that the amount of ammonia that is desorbed is minimal,[7,9,13,23] and several experimental studies suggested that nitrogen insertion is possible before desorption processes occur.[1,2,6,8,26,27] Most experimental studies used x-ray photoelectron spectroscopy (XPS) as the main characterization technique,[1–3,6,10,12,16,18–20,54] and the lack of high-resolution investigations was partially responsible for the controversy regarding the thermal decomposition of ammonia. The difficulty in resolving the N 1*s* signatures arises from the fact that the binding energies of various N-containing structures on the Si(100) surface differ by only about 1.2 eV in the 300–900 K temperature range. Recently, Kim *et al.* used high-resolution XPS to study the thermal decomposition of ammonia on Si(100),[26,27] showing that a Si(100) surface exposed to NH_3 at room temperature and annealed to 550 K has several different species present, including $(Si)NH_2$, $(Si)_2NH$, and $(Si)_3N$, in comparable concentrations. This work demonstrated that the decomposition of ammonia occurs before desorption takes place, in disagreement with the cited theoretical studies. Previous experimental investigations using high-resolution electron energy loss spectroscopy (HREELS) have suggested that decomposition takes place below 600 K and, more importantly, that the $(Si)_2NH$ species are mainly backbonded,[8,11] instead of bridged structures, which are suggested to be the main product from most theoretical considerations.[48,51] Angle-dependent XPS experiments conducted by Kim and Yeom[27] seem to confirm the preference of the subsurface insertion as opposed to surface insertion. A theoretical study that supports the formation of backbonded structures was conducted by Xu *et al.*,[49] but in this investigation, the cluster representing the silicon surface was fully relaxed and therefore did not represent realistically the constraints of a solid crystal. However, the comparison of results in Ref. 48 to those in Ref. 49 offers an important clue: If the constraints present on the surface are attenuated, the decomposition of ammonia would turn into a more facile, favored process.[14,19] A simple analysis, based on the average bond energies of N-H and Si-Si vs. Si-N and Si-H,[32] confirms that this direction is worth exploring.

As can be noted from the description above, the majority of the experimental studies involving the system $NH_3/Si(100)$ relies on XPS,[1–3,6,10,12,16,18–20,26,27,54] TPD,[1,7,9,13,14,23,47] STM,[4,5,25,28–30] or HREELS.[8,11,14,23] However, a powerful surface analysis technique such as infrared (IR) spectroscopy has rarely been used to investigate this system. To the best of our knowledge, there are only two previous IR studies, those reported by Queeney *et al.* on the cryogenic adsorption of ammonia as function of the coverage[24] and by Dillon *et al.* on thermal decomposition of ammonia on porous silicon.[55] As demonstrated in these previous studies, the Si-H stretch vibration is highly sensitive to the neighboring species, shifting its maximum intensity over a range that can be as large as 20 cm^{-1}. Thus, infrared spectroscopy exhibits very high sensitivity toward the chemical environment for the study of the $NH_3/Si(100)$ system. In the present investigation, the combination of infrared spectroscopy with density functional calculations is employed to in-

vestigate the adsorption and decomposition of ammonia in a temperature range of 300–800 K. This span is particularly interesting because most modern applications require moderate temperature regimes, not only to produce ultrathin films through atomic layer deposition[56–58] but also as a way to functionalize the semiconductor surface for applications in molecular electronics and design of self-assembled surface structures.[59,60] The results and their interpretation are divided into three sections. In the first section, spectroscopic results corresponding to adsorption at room temperature are analyzed and compared to computational results, obtaining evidence of the presence of various long-range configurations of adsorbates. In the second section, vibrational frequencies, both predicted and experimental, are compared to gain some insight into the thermal decomposition of surface species. Our results suggest that nitrogen insertion is possible at temperatures lower than those required for desorption processes to take place and that the bridged structure (and therefore the surface insertion pathway) does not seem to play a determining role, contrary to what was predicted previously. In the last section, we offer a theoretical explanation for the ease of insertion, finding that the long-range configuration of back-bonded structures mitigates the surface strain imposed upon insertion. We discuss the implications of our results not only in terms of the formation of NH_X structures on a Si(100) surface but also considering the potential future applications of this system.

II. EXPERIMENTAL AND COMPUTATIONAL METHODS

A. Experimental details

The experiments were carried out in an ultrahigh vacuum (UHV) chamber, located at the University of Delaware. This UHV chamber operates at a base pressure of less than 10^{-9} torr and is equipped with a mass spectrometer (SRS 200), a setup for Auger electron spectroscopy (AES), an ion gun for surface sputtering and an infrared spectrometer (Nicolet 560). The trapezoidal Si(100) sample ($25\times20\times1$ mm^3, 45° beveled angles) was provided by Harrick Scientific. The surface was prepared by argon (Matheson, 99.999%) sputtering and annealing cycles until the cleanness of the surface was confirmed with AES. Annealing of the surface to temperatures above 1100 K is possible through an e-beam heater (McAllister Technical Services). The temperature of the silicon substrate was measured by a K-type thermocouple wedged between an isolating ceramic sleeve and the silicon surface. The accuracy of the thermocouple reading was confirmed by calibration with the hydrogen desorption from a clean Si(100) crystal observed at 800 K. The clean Si(100)-2×1 surface obtained through this procedure was exposed to NH_3 (Air Products, anhydrous grade) at room temperature and briefly annealed *in situ* to temperatures in the range of 300–800 K. The typical exposure of ammonia was 100 L (1 L$=10^{-6}$ torr s), which was found to be sufficient to guarantee the saturation of the Si(100) surface. The purity of argon and ammonia was confirmed in situ by mass spectrometry. The IR spectrometer was coupled to an external liquid-nitrogen-cooled mercury cadmium telluride detector, and each spectrum consisted of 2048 scans, with a resolution of 4 cm^{-1}. The trapezoidal geometry of the Si sample allowed the collection of spectra using the multiple internal reflection mode at 300 K, the temperature at which the background spectrum of a clean silicon surface was collected. Multiple internal reflection increases the sensitivity of surface vibrations, but at the cost of reducing the spectroscopic window to wave numbers above ~1500 cm^{-1} at room temperature. Thus, we are sacrificing the characteristic NH_2 scissoring mode (~1530 cm^{-1}) in order to improve the Si-H stretch signal (~2000–2200 cm^{-1}). This offers a strategic advantage in this study, since the Si-H stretch signal is observed to be more intense than other possible informative signals, such as the N-H stretch and the NH_2 scissoring mode. According to the theoretical prediction for structure D1 described in Fig. 2, the intensity of the $\nu_{\text{Si-H}}$ absorption band is approximately 2.5 times stronger than that of the NH_2 scissoring mode and approximately five times stronger than $\nu_{\text{N-H}}$ mode. This comparison is also in agreement with the experimental studies of Queeney *et al.*[24] Despite the fact that for some systems the spectroscopic window can be expanded below 1500 cm^{-1}, in this case, the small intensity of the NH_2 scissoring mode makes the measurement of this feature less reliable than that of the Si-H stretching mode. In addition, decomposition of (Si)NH_2 species originates the decrease and disappearance of the N-H vibrations, while the Si-H vibrational intensity increases.[8,11,55] The work of Dillon *et al.* confirms this fact and also shows that N-H scissoring modes do not show any significant change upon surface transformation, while the Si-H vibrational mode shows an overall blueshift of the signal.[55]

B. Computational methods

Three models were used to represent the (100) surface, which represent one, two, or three surface dimers of the same row (Si_9H_{12}, $Si_{15}H_{16}$, and $Si_{21}H_{20}$, respectively). For all clusters, the silicon atoms representing the top two layers of the silicon single crystal and all the atoms representing the adsorbates were allowed to relax, while the remaining atoms were held at fixed coordinates, simulating lattice conditions. Density functional calculations were performed using the B3LYP method[61,62] with the 6-31+G(d) and the 6-311+G(d,p) basis set as implemented in the GAUSSIAN 03 set of programs.[63] While the 6-31+G(d) basis set was chosen for calculations involving all three cluster models, the computationally more expensive 6-311+G(d,p) basis set was employed only for one-dimer clusters. In order to prove the sufficiency of the 6-31+G(d) basis set, Table I shows the values obtained for potential energy surfaces corresponding to surface insertion and subsurface insertion using a one-dimer cluster (Fig. 2) and compares them to the values reported by Widjaja and Musgrave (Ref. 48), where a larger basis set was used. A high degree of consistency is found not only for the dissociatively adsorbed structure D1 but also for the structures and transition states involved in the surface insertion pathway. However, the values corresponding to subsurface insertion are found to differ significantly. These two facts suggest that there is a good agreement with our level of theory and more sophisticated basis sets and that the

TABLE I. Energetic values (kJ/mol) obtained for the first step of surface and subsurface insertion (D1→B1 and D1→S1, respectively) at the B3LYP/6-31+G(*d*) level of theory, as compared to Ref. 48, where the B3LYP/6-311++G(2*d*,*p*) level of theory was used. For both studies, values are with respect to reactant level (NH_3+empty cluster).

	D1→B1		D1→S1	
	This work	Ref. 48	This work	Ref. 48
Si-NH_2	−223.4	−218.2	−223.4	−218.2
TS1	20.6	17.4	−10.2	12.6
$(Si)_2NH_2$	−132.3	−116.8	−118.7	−60.2
TS2	26.6	42.5	49.3	112.9
$(Si)_2NH$	−260.3	−238.4	−249.7	−179.7

observed differences might arise from specific constraints imposed on the models in the theoretical work of Widjaja and Musgrave.[48] It will be observed in this work that differences in theoretical results also arise from the type of model cluster (Si_9H_{12}, $Si_{15}H_{16}$, or $Si_{21}H_{20}$) used in the calculations.

Vibrational frequencies were predicted for all the models considered using the 6-311+G(*d*,*p*) basis set for one-dimer cluster models and using 6-31+G(*d*) basis set for models involving the two- and three-dimer clusters. In order to avoid systematic errors, two correction factors were used to scale the predicted wave numbers: 0.955 476 and 0.950 826 for the 6-311+G(*d*,*p*) and the 6-31+G(*d*) basis sets, respectively. These factors were obtained by comparing experimental and calculated values for the Si-H stretch vibrations in a monohydrogenated Si(100) surface, similar to our previous strategies.[64,65]

C. Simulation of spectra and fitting procedure

Since most models presented in this study exhibit more than one vibrational feature in the Si-H stretch frequency range, the sole prediction of a vibrational frequency may not be sufficient to visualize the contribution of a specific structure to the experimental signal. Multiple vibrational modes would influence both the maximum intensity and the shape of the predicted absorption signal. Thus, in addition to the calculation of vibrational frequencies for every structure considered in this investigation, we simulated its corresponding spectrum. We started the process of simulation by taking into account a predicted vibrational frequency and its intensity. We chose a Gaussian distribution for each predicted frequency, with a full width at half maximum (FWHM) constant for each vibrational mode. Since our group has previously reported a variety of spectroscopic investigations on Si(100), we searched for a set of experiments with a single Si-H vibrational mode. Such a measurement would offer an indication of how a Si-H vibration broadens under our experimental conditions. The chosen system was ethyl iodide on Si(100), which leads to the formation of the H-Si-Si-I species on this surface.[64,66] Due to the bulkiness of the halogen and ethyl groups, the adsorption was found to occur on every other silicon dimer within a dimer row, and upon thermal annealing, hydrogen and iodine atoms paired up on the same silicon dimer to form the H-Si-Si-I entity. The FWHM value found for the Si-H vibration was found to be 19 cm^{-1}, and this value was used for all vibrations predicted in this study. The maximum intensity of a Si-H mode for each structure was represented as 100%, and the other modes within the same structure were scaled accordingly. Far from being used quantitatively, these simulated spectra are intended to provide some additional help in visualizing possible contributors to the experimental spectra.

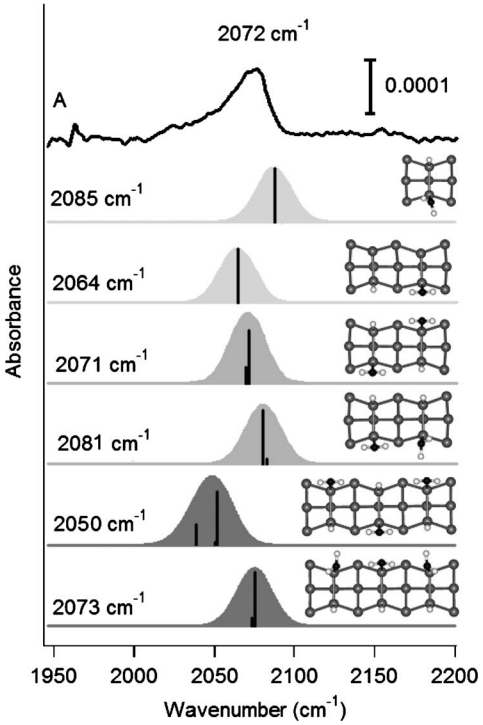

FIG. 3. Infrared spectrum of the Si(100) surface after exposure of 100 L NH_3 at room temperature (A), together with predicted vibrational modes and simulated spectra corresponding to dissociatively adsorbed NH_3 on Si(100). From top to bottom, simulated curves corresponding to structure D1, as calculated from a one-dimer cluster, interdimer dissociation in a two-dimer cluster, alternate configuration using a two-dimer cluster, aligned configuration using a two-dimer cluster, alternate configuration using a three-dimer cluster, and aligned configuration using a three-dimer cluster. Frequencies calculated at the B3LYP/6-31+G(*d*) level of theory. As indicated in the experimental section, a factor of 0.953 535 is used to scale the predicted values. Black, nitrogen; gray, silicon; white, hydrogen.

III. RESULTS AND DISCUSSION

A. Dissociative adsorption at room temperature

The vibrational spectrum obtained after saturation of the surface with ammonia at room temperature is shown in Fig. 3. The maximum intensity of the Si-H stretch vibration is located at 2072 cm^{-1}, in agreement with previous studies of adsorption of ammonia on silicon surfaces at room temperature,[8,11,55] as shown in Table II. It is apparent from the experimental signal at room temperature that small con-

TABLE II. Experimental and theoretical values for the vibrational modes corresponding to the Si-H stretching mode produced upon dissociative adsorption of NH_3 on a silicon surface. One-dimer and two-dimer calculations at the B3LYP/6-311+G(d,p) and B3LYP/6-31+G(d) levels of theory, respectively.

	System	Frequency (cm^{-1})
	Experimental	
Ref. 23	Si(100), 110 K	2050
Ref. 24	Si(100), 220 K	2055, 2078
Ref. 55	Porous Si, 300 K	2077
Ref. 8	Si(100), 300 K	2078
Ref. 11	Si(100), 300 K	2073
This work	Si(100), 300 K	2072
	Theoretical (DFT)	
Ref. 24, aligned	Two-dimer cluster	2073, 2077
Ref. 24, alternate	Two-dimer cluster	2057, 2059
This work, one dimer	One-dimer cluster	2084
This work, aligned	Two-dimer cluster	2080, 2083
This work, aligned	Three-dimer cluster	2068, 2073, 2075 [2070][a]
This work, alternate	Two-dimer cluster	2069, 2071
This work, alternate	Three-dimer cluster	2038, 2050, 2051 [2041][a]

[a]The numbers in square brackets indicate the predicted frequency for the three-dimer cluster model without considering coupling effects, that is, when Si-H species on the sides where replaced by Si-D.

tributions extend the absorption signature toward lower wave numbers. These small contributions were pervasive through different sets of experiments and overall were consistent with the position of the Si-H signal observed upon adsorption at lower temperatures.[23,24] Queeney *et al.* have previously assigned a signal at 2055 cm^{-1} to an alternate adsorption, while a signal at 2073–2078 cm^{-1} was suggested to correspond to an isolated configuration, observed only at low coverages.[24] In order to gain some insight into the possible long-range configurations, we performed frequency calculations for both the alternate and the aligned configurations using two- and three-dimer clusters as surface models. In addition, we include the predicted frequency for a one-dimer cluster with one dissociated ammonia molecule. The results of these predictions are summarized in Table II. Figure 3 shows the simulated spectra for each model. In agreement with Queney *et al.*,[24] we found that the predicted Si-H vibrational frequency is greatly affected by the neighboring species. Moreover, our study shows that the predicted difference between aligned and alternate configurations depends on the number of neighbors that are involved in a computational simulation. When one neighbor is considered (two-dimer cluster models), the predicted frequencies for the aligned and alternate configurations are found to generate simulated spectra centered around 2081 and 2071 cm^{-1}, respectively. When two neighbors are considered (three-dimer cluster), the simulated spectra for aligned and alternate configurations are centered on 2073 and 2050 cm^{-1}, respectively. If the two Si-H species neighboring to the central dimer are replaced by deuterium to exclude coupling effects, a single signal is produced at 2070 cm^{-1} (for the aligned configuration) and 2041 cm^{-1} (for the alternate configuration). These values contrast with the predicted frequency obtained using a one-dimer cluster as a model (2085 cm^{-1}), showing the capital influence of neighboring dimers on the vibrational features on the surface. The origin of this influence can be explained in terms of the presence of $(Si)NH_2$ species, specifically how it affects the polarization of the Si atom in the Si-H moiety. Using the three-dimer cluster in the alternate configuration as an example, it is expected that the two $(Si)NH_2$ groups neighboring the central Si-H bond modify the electronic density around the central Si atom. The attachment of an NH_2 group to a Si atom produces a positive polarization in this atom, which, in turn, polarizes negatively the silicon atom in the neighboring dimer that is aligned to the $(Si)NH_2$ moiety. This effect is less significant for the two-dimer cluster model, because of the presence of only one neighbor, and is absent in the one-dimer model. The negative polarization of the silicon atom in the Si-H moiety, induced by neighboring $(Si)NH_2$ species, weakens the Si-H bond and redshifts its stretching mode from 2085 cm^{-1} for a non-neighbor model to 2071 and 2050 cm^{-1} as one and two neighbors are considered, respectively. In contrast, vibrational frequencies corresponding to the aligned configuration show a redshift to only 2081 and 2071 cm^{-1} when one and two neighbors are considered, respectively. In this case, it could be proposed that electronic effects from the neighbors do not induce a negative polarization of the Si atom in the Si-H moiety as dramatically as in the previous case. In addition, the decreased effect of polarization can be originated from the possibility of a "gauche"[39] orientation of two $(Si)NH_2$ entities, which may lead to the formation of hydrogen bridges, as observed in the alternate configuration in Fig. 1.[24,39–41,67] These intermolecular interactions redirect the electronic density toward the H atoms in the central $(Si)NH_2$ group, instead of distributing it along the surface. It is important to mention

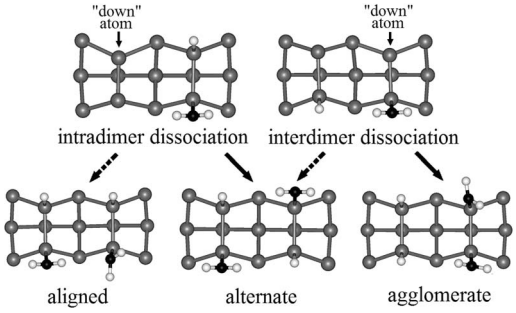

FIG. 4. Products of intradimer and interdimer dissociative adsorption of NH_3 on an empty Si(100) surface. Optimized models at the B3LYP/6-31+G(*d*) level of theory show the buckling of the unoccupied surface atoms. Upon adsorption and dissociation of another NH_3 molecule, three long-range configurations can be expected. For both initial structures, solid arrows lead to the most likely product, and dashed arrows lead to the least likely products, considering the adsorption as a nucleophilic attack to the down atom. Black, nitrogen; gray, silicon; white, hydrogen.

that the formation of hydrogen bridges also reduces adsorbate-adsorbate repulsion forces between aligned $(Si)NH_2$ entities.[39,46] By considering both induced polarization and hydrogen bonding, we obtain a simplistic model able to offer a qualitative explanation of the remarkable dependence of the Si-H stretch vibrational frequency on the number and the nature of the neighbors. It is worth noting that the use of a three-dimer cluster might introduce some inaccuracies in this configuration, since the orientation of the two $(Si)NH_2$ species located on the first and third dimer of the cluster is directed toward the central Si-H species (Fig. 1), which could be simulated in a different fashion in a periodic (slab) system.[39,40]

Since in all cases the alternate configuration produces a vibrational Si-H stretch signal that is redshifted with respect to the signal from the aligned configuration, our theoretical results suggest that the aligned structure is more abundant on the surface. A recent STM investigation has shown that both configurations are present on the surface, forming "chains" that can prefer one of these configurations.[28] This observation makes the analysis of the spectrum more complex, since in the event that two chains with different configurations approach each other, the Si-H vibrations at the border will produce different vibrational signatures as well. In addition, as it was stated in Sec. I, recent investigations suggest that the dissociation of ammonia can also be interdimer.[15,29,30,41–43] Figure 4 shows the interdimer and intradimer dissociation species, together with the most likely product of a second dissociation as a new ammonia molecule is adsorbed on the surface, under the consideration that the electron pair of the upcoming molecule will attack the most electrophilic (down) surface atom available. While in the case of the intradimer dissociation this would lead to an alternate configuration, the result from the interdimer dissociation would be a third configuration where two $(Si)NH_2$ species are present in the same dimer (hereafter called *agglomerate* configuration). These multiple configurations can potentially be all present on the surface at 300 K as the thermal energy is sufficiently high and the dynamic buckling of surface dimers may make multiple surface reaction sites accessible, while other effects (such as hydrogen bridging, adsorbate-adsorbate repulsion, etc.) also have to be considered.[46]

Predicted adsorption energies for all the structures containing $(Si)NH_2$ species are summarized in Table III. Energies corresponding to intradimer and interdimer dissociations on the two-dimer cluster are found to be −238.5 and −170.8 kJ/mol, respectively, showing a larger difference between these two dissociation products than in previous investigations,[29,41,43] although the energy corresponding to the interdimer dissociation product is in good agreement with these previous calculations. The three possibilities for a saturated surface (aligned, alternate, and agglomerate) have adsorption energies of −234.2, −231.7, and −231.4 kJ/mol, respectively. The similar stability for the three configurations suggests that the formation of one configuration or the other is not under thermodynamic control. However, the formation of a long-range agglomerate configuration can be expected to be sterically hindered, leaving the other two configurations (aligned and alternate) as major components. Since Queeney *et al.* observed that the position of the Si-H vibrational frequency is close to 2078 cm^{-1} at low coverages, shifting to 2055 cm^{-1} upon saturation,[24] we performed experiments with successively higher doses of ammonia, up to 400 L. Such large exposure did not significantly affect the position

TABLE III. Predicted adsorption energies (kJ/mol) corresponding to dissociatively adsorbed NH_3 on the Si(100), considering both unsaturation and saturation of the model surface. In all cases, the values are given with respect to reactants (NH_3 and the empty Si cluster) at the B3LYP/6-31+G(*d*) level of theory.

	This work (DFT)	Ref. 29 (slab)	Ref. 44 (slab)	Ref. 28 (slab)	Ref. 46 (slab)
			Unsaturated layer		
Intradimer	−238.5	−198.8	−191.1		
Interdimer	−170.8	−172.8	−166.0		
			Saturated layer		
Alternate	−231.7			−197.3	−202.7
Aligned	−234.2			−197.3	−196.7
Agglomerate	−231.4				

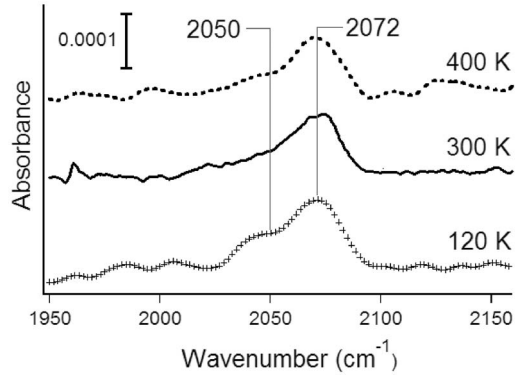

FIG. 5. IR spectra obtained after the exposure of the Si(100) surface to 100 L NH_3 at 120 K (line with markers), 300 K (solid line), and 400 K (dashed line). While a vertical line at 2072 cm^{-1} indicates, in all cases, the most prominent feature, adsorption at 120 K results in the enhancement of a minor component at lower wave numbers, around 2050 cm^{-1}, in agreement with Refs. 23 and 24.

of the Si-H signature, confirming that saturation had been reached and that 2072 cm^{-1} is the position of the Si-H vibrational frequency corresponding to the room temperature adsorption of NH_3 on Si(100). It is apparent that the aligned configuration is present at this temperature, since experimental observations agree well with the predicted ν_{Si-H} absorption signature for such configuration (2072 cm^{-1} in this work, 2073 cm^{-1} for Larsson *et al.*,[11] and 2078 cm^{-1} for Fujisawa *et al.*[8]). On the other hand, at cryogenic temperatures, the alternate configuration may be preferred on the surface, as demonstrated by the fact that the predicted frequency for such a configuration (2050 cm^{-1}) agrees with the experimental results of Queeney *et al.*[24] (2055 cm^{-1}) and Bater *et al.*[23] (2050 cm^{-1}). This observation is substantiated by recent STM investigations of ammonia on Si(100) at relatively high coverages. While upon adsorption at 65 K the alternate configuration has been observed,[25] an STM investigation, carried out at room temperature, found both configurations on the surface.[28] A recent theoretical work supports the temperature dependence of the long-range ordering by considering the influence of the hydrogen bridging between a $(Si)NH_2$ entity and an incoming NH_3 molecule, which favors the aligned configuration.[45,46] Once the formation of the aligned structure has begun, hydrogen bonding stabilizes the adsorbed layer.[28,39] In order to investigate this temperature dependence, adsorption of NH_3 was performed at three different temperatures: 120, 400, and 300 K (room temperature), as summarized in Fig. 5. The experimental Si-H stretch vibrational signature contains two major components, likely corresponding to the alternate and aligned configurations, whose predicted vibrational spectra (using three-dimer clusters) were located around 2050 and 2072 cm^{-1}, respectively. The approximate ratio of the observed absorption intensities is 1:3 (alternate:aligned) for the adsorption at 300 K and is 1:2 (alternate:aligned) for the adsorption at 120 K. Thus, the feature located at lower wave numbers, assigned to the alternate configuration, is obviously favored when adsorption occurs at cryogenic temperatures,

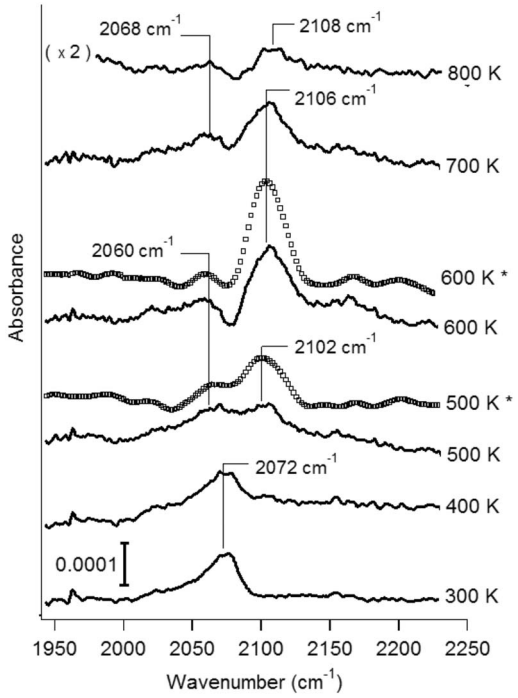

FIG. 6. IR spectra obtained upon annealing of the ammonia-covered surface deposited at 300 K. The annealing temperature and major intensities are indicated for each spectrum. Spectra obtained from flash annealing are shown by solid lines, while spectra obtained after 1 min annealing are shown with markers (□).

which is in agreement with previous experimental results at 110 and 220 K (Refs. 23 and 24, respectively), as summarized in Table II. The experimental results of Fig. 5 clearly show that ammonia adsorption on Si(100) is temperature dependent, although it is not possible to offer anymore definitive quantification of the preferred configuration on the surface, as the vibrational intensities from these two configurations may not be exactly proportional to the fractions of adsorbates and, as discussed above, other configurations can be potentially present on the surface.

Although a three-dimer cluster might be a better representation of the surface because it shows the influence of two neighbors, the theoretical analysis of our experimental results in the next section would be computationally expensive if such a large cluster is used as a model. Thus, we will represent the surface by using a two-dimer cluster. The alternate configuration will be employed, because it offers the possibility of studying three different configurations for subsurface migration, as will be explained below. In addition, it will be shown that this configuration dependence of the Si-H vibrational frequency is not as crucial for $(Si)_2NH$ species as it was for the $(Si)NH_2$ species discussed in this section.

B. Thermal decomposition in the temperature range 300–800 K

Figure 6 shows the change of the Si-H stretch region of the spectra as the surface is annealed to temperatures in the range of 300–800 K. As expected, the Si-H vibrational mode is highly sensitive to surface transformations and shows a

significant blueshift of the maximum intensity from 2072 to 2108 cm^{-1}. Upon annealing to 400 K, there is no considerable change, but at 500 K and above, there is a significant change both in the position and in the intensity of this absorption feature. Two factors may be responsible for this: (a) the proximity of a nitrogen atom to a Si-H bond (common to all decomposed structures shown in Fig. 2), which induces a positive polarization of the Si atom in the Si-H moiety, increasing the strength of the Si-H bond, and (b) the formation of dihydride silicon species (as for structures B2 and S2). The increase of the area corresponding to the Si-H stretch absorption feature is straightforwardly attributed to the presence of a larger number of Si-H bonds; however, the presence of the more electronegative N atom in the proximity of the Si-H bond can also affect this increase, as described previously by a theoretical investigation for the $H_2O/Si(100)$ system.[68] The absorption signature at 500 K shows two main Si-H stretch components, centered around 2060 and 2102 cm^{-1}. These components are present at higher temperatures as well, but a progressive blueshift is observed. At 700 K, the main components of the vibrational signal are centered around 2068 and 2106 cm^{-1}, and a very small intensity of these two features can be observed even after flash annealing to 800 K. The maximum intensity of the signal is reached at 600 K. At 700 and 800 K, a decrease of the intensity, undoubtedly associated with desorption of surface species, is observed. As cited in Sec. I, TPD experiments have found that ammonia desorbs at 650 K, while hydrogen evolves from the surface at 780 K, resulting in the removal of all H-containing species.[7,9,13,14,23,47] In summary, our experiments demonstrate that decomposition of $(Si)NH_2$ species is possible at temperatures lower than those required for the desorption of ammonia and/or hydrogen.

To further understand the decomposition of adsorbed species, spectra obtained upon 1 min annealing of the saturated surface at 500 and 600 K were also collected and are included in Fig. 6. In these cases, the blueshifted component of the Si-H stretch region appears to be more dominant than in flash-annealing studies. In order to gain some insight into the nature of the decomposed species, we carried out frequency calculations for the structures corresponding both to the surface and to the subsurface nitrogen insertion pathways.

The surface models considered in this section consist of a two-dimer cluster with two ammonia molecules dissociated in the alternate configuration. This represents an interesting model because of the multiple possibilities for some of the decomposed species. Figure 2 has shown the proposed pathways for surface and subsurface insertions. Due to the lower degree of symmetry, structures B2 and S1 can be formed in three different configurations, which are shown in Fig. 7. These configurations will be called hereafter *in-in*, *out-out*, or *in-out*, depending on whether the N insertion occurs inward or outward with respect to the C_2 rotational axis of an unoccupied silicon two-dimer cluster. Frequency calculations were performed for the optimized models corresponding to the structures shown in Figs. 2 and 7, considering both the one-dimer and two-dimer clusters, and each possible configuration based on structures B2 and S1 was included. Figure 8 shows the simulated spectra for each structure and/or configuration, following the procedure described in Sec. II C,

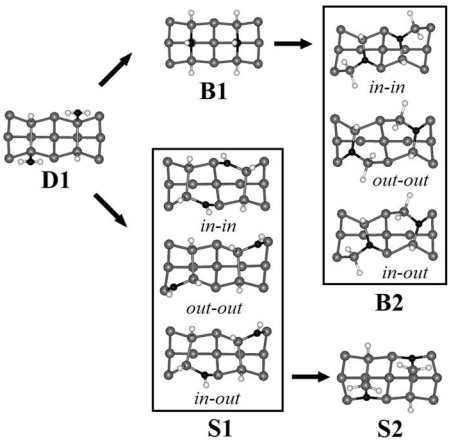

FIG. 7. Possible configurations for decomposed structures S1 and B2 using, as a starting model, a two-dimer cluster with two dissociatively adsorbed NH_3 molecules in the alternate configuration. Due to their high symmetry, structures D1, B1, and S2 have only one possible configuration. Black, nitrogen; gray, silicon; white, hydrogen.

and predicted frequencies and intensities leading to these simulated spectra are shown in Table IV. With the exception of structure S2, decomposed structures do not have a pronounced change in their predicted spectra as a function of the model cluster size. Thus, the cluster size does not seem to affect the position or shape of the simulated spectra to a significant extent, although for the two-dimer cluster models representing backbonded structures based on a S1-type con-

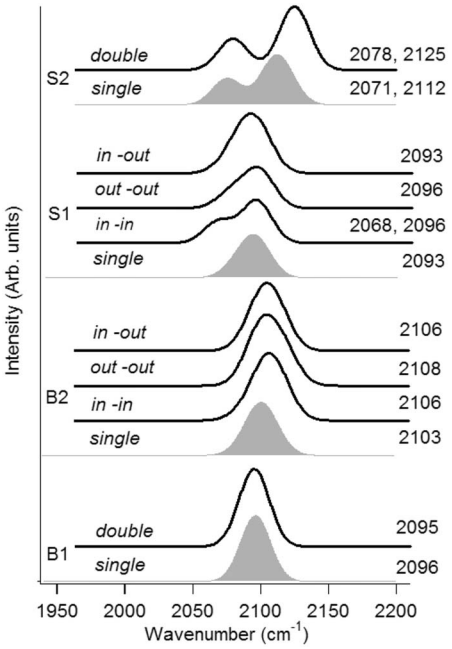

FIG. 8. Simulated spectra corresponding to decomposed structures, as predicted at the B3LYP/6-31+G(*d*) level of theory. For each structure, both the one-dimer and the two-dimer cluster were used to predict the vibrational modes (denoted by single and double, respectively). For structures with multiple configurations (S1 and B2), the simulated spectra for each configuration are presented.

TABLE IV. Predicted frequencies for $(Si)_2NH$ and $(Si)_3N$ structures discussed in this work. One-dimer and two-dimer cluster calculations at the B3LYP/6-311+G(d,p) and B3LYP/6-31+G(d) levels, respectively. The numbers in square brackets correspond to the calculated intensities for the respective vibrations.

Structure	Frequency, cm^{-1} [intensity]
B1, one-dimer	2095 [90], 2097 [100]
B1, two-dimer	2089 [19], 2091 [21], 2095 [88], 2097 [100]
B2, one-dimer	2089 [12], 2099 [100], 2108 [58]
B2, two-dimer (in-in)	2088 [4], 2090 [20], 2103 [35], 2104 [100], 2116 [33], 2116 [44]
B2, two-dimer (out-out)	2095 [1], 2097 [65], 2099 [9], 2102 [100], 2108 [61], 2119 [98]
B2, two-dimer (in-out)	2091 [2], 2093 [16], 2100 [28], 2103 [100], 2112 [41], 2114 [45]
B3, one-dimer	2085 [100]
S1, one-dimer	2083 [43], 2096 [100]
S1, two-dimer (in-in)	2068 [28], 2069 [35], 2095 [21], 2096 [100]
S1, two-dimer (out-out)	2077 [19], 2079 [27], 2092 [9], 2098 [100]
S1, two-dimer (in-out)	2075 [26], 2082 [39], 2089 [81], 2098 [100]
S2, one-dimer	2071 [76], 2109 [100], 2118 [56]
S2, two-dimer	2077 [35], 2080 [55], 2115 [3], 2122 [100], 2128[89], 2132 [1]

figuration, a small shoulder can be observed for configuration in-in, which is absent for out-out and in-out configurations.

Previous theoretical studies have suggested that formation of B1 might be the most facile insertion mechanism.[48,51] Upon decomposition, structure B3 (Fig. 2) was proposed to follow the formation of structure B1.[48,49] For such a structure, the Si-H stretch vibration on a one-dimer cluster was predicted to be around 2085 cm^{-1} [at the B3LYP/6-311+G(d,p) level of theory]. Thus, this pathway would indicate that upon annealing, the maximum intensity blueshifts to 2095 cm^{-1}, and once desorption processes start, the signal would redshift back to 2085 cm^{-1}, which disagrees with our experimental profile. Similarly, Kim and Yeom did not find evidence of structure B3 in their XPS study,[27] supporting their results with a theoretical investigation of core-level shifts during NH_3 decomposition.[69] Thus, in order to explain further dissociation of B1, we have considered structure B2, which corresponds to the complete decomposition of ammonia on Si(100) through the D1-B1-B2 sequence. According to our prediction of vibrational frequencies, this pathway would exhibit the initial blueshift toward 2095 cm^{-1}, followed by another blueshift that would bring the maximum intensity to wave numbers around 2105 cm^{-1}. This behavior partly agrees with the temperature profile shown in Fig. 6, except for the apparent existence of two features at 700–800 K. At this point, it is worth describing the behavior of the redshifted component observed in the 500–800 K range. This component decreases its intensity from 500 to 600 K without changing its position (around 2060 cm^{-1}), but as the temperature increases to 700 K the intensity of this feature increases as well, and the position is slightly blueshifted to 2068 cm^{-1}. It is likely that the decrease occurs as a result of the conversion or desorption of $(Si)NH_2$ species and that the formation of new species is responsible for the rise of the signal at 2068 cm^{-1}. This view is supported by the fact that $(Si)NH_2$ structures are known to be completely transformed in the 700–800 K range.[6–9,13–15,23,27,47] The presence of two features can be explained by considering the subsurface structure S2. As a matter of fact, the relative intensities of the two components observed at 700 and 800 K resemble the relative intensities predicted for such structure quite well. Although no definitive proof can be obtained from the comparison of the predicted vibrational frequencies with the experimental ones, it is possible to infer that the position of the peak above 2100 cm^{-1} has two different sources. On one hand, it could be almost exclusively due to the presence of structure B2, which would indicate that $(Si)_2NH$ structures are easily decomposed once they are produced on the surface. On the other hand, this peak can be the result of a mixture of $(Si)_2NH$ structures with S2, where contribution of the latter to the overall spectral signature increases with temperature, as evidenced by the continuous blueshift to 2108 cm^{-1}. Nevertheless, in both cases, the blueshift can only be explained by the presence of the $(Si)_3N$ structures on the surface at temperatures as low as 500 K.

The thermodynamic stabilities of the decomposed structures considered here are shown in Table V. In order to explain the stability trends, we first have to take into account the presence of unconstrained atoms in the cluster models. These unconstrained atoms include the silicon dimer atoms, the silicon atoms in the second layer, and four hydrogen atoms representing silicon surface atoms from two neighboring dimers along the same row. These hydrogen terminations are connected to only one silicon atom in the cluster and, therefore, are able to move more freely in the course of optimization procedures compared to the surface silicon atoms

TABLE V. Energies of structures corresponding to both pathways of decomposition [kJ/mol, at the B3LYP/6-31+G(*d*) level] using as a model surface the two-dimer cluster. The effect of the configuration (for structures B2 and S1) is included. In all cases, the values are given with respect to reactants (NH_3 and the empty Si cluster).

	This work		Ref. 48	Ref. 49	
	One-dimer 6-311++G(*d*,*p*)	Two-dimer 6-31+G(*d*,*p*)	B3LYP 6-311++G(2*d*,*p*)	B3LYP 6-31G**	Ref. 51 (slab)
D1	−223.4	−231.7	−213.2	−222.2	−189.4
		Surface insertion pathway			
B1	−260.3	−265.6	−238.3	−272.0	−217.1
B2	−207.5	−201.8 (in-in)			
		−192.5 (out-out)			
		−175.2 (in-out)			
B3	+35.1			−64.0	
		Subsurface insertion pathway			
S1	−249.7	−224.3 (in-in)	−175.6	−268.6	−164.1
		−255.4 (out-out)			
		−233.6 (in-out)			
S2	−285.1	−260.2	−129.3	−314.6	−141.9

they represent. Since the presence of these hydrogen terminations in the cluster model will be recurrently cited below, we will refer to these entities as H_{surf} to highlight their role as representation of neighboring Si surface atoms. The importance of these H_{surf} entities resides in the fact that the strain directed toward these terminations is easily dissipated. A one-dimer cluster model has four H_{surf} per dimer, while a two-dimer cluster model has two H_{surf} per dimer. Structures corresponding to N insertion are expected to show more stability in the one-dimer cluster, especially for structures that are expected to heavily modify the surface structure (Table V). For structures S1 and B2 represented using the two-dimer cluster, it is observed that the thermodynamic stability depends on the configuration. In principle, the higher stability of the configuration out-out for structure S1 and configuration in-in for structure B2 can be attributed to the fact that in these structures, the strain imposed by the insertion is directed toward H_{surf} entities. However, other possibilities for strain relief have to be considered to explain the stability of a configuration. In the case of B2, for example, while the configuration in-out directs the strain of one of the insertions toward the H_{surf} entities, the configuration out-out does not have such a possibility for strain relief. Despite this fact, the stability of the configuration out-out is higher than the in-out, which is explained by strain cancellation, as the insertion of one nitrogen atom is compensated by a symmetrical insertion of a nitrogen atom on a neighboring dimer. From the level of distortion of the in-out configuration (Fig. 7), it is possible to infer that this structure is under the effect of a marked strain, and thus, in this case, the fact that one N atom moves in the outward direction (toward H_{surf} entities) imposes even more strain onto the silicon lattice. On the other hand, the out-out structure gains some stability because nitrogen atoms move in the opposite directions upon insertion, diminishing the strain by cancellation, as can be observed from the fact that the resulting structure does not seem to be as distorted as the in-out configuration. Similar behavior can be deduced from configurations of structure S1, where the in-in configuration is almost as stable as the in-out configuration. Therefore, it is possible that species containing adsorbates undergoing subsurface insertion *can gain stability* if the long-range arrangement is such that the strain produced by the insertion is mitigated. Previous studies using one-dimer clusters could not have investigated this possibility.[48,49] This idea will be further developed in the next section. Before proceeding to this comparison, the thermodynamic data obtained here will be contrasted with our spectroscopic findings to gain more insight into the nature of decomposed species.

Our spectroscopic results showed that the simulated spectra corresponding to structure B2 match nicely with the experimental observations. However, under thermodynamic considerations, the formation of B2 is not favorable, as the formation of B2 from B1 represents an endothermic process where the product is 50–90 kJ/mol less stable than the starting structure (depending on the cluster model used, as can be seen in Table V). Structure B1 cannot be ruled out either spectroscopically (because its predicted frequency is similar to the one corresponding to S1 and they cannot be resolved in our experiments) or thermodynamically (because it is one of the most stable structures according to our computational data). However, none of its possible decomposed products (B2 and B3) has been found to be present on the surface through this study: Structure B2 is not stable thermodynamically and structure B3 has a vibrational signature that is not observed experimentally. Under thermodynamic considerations, the first step of subsurface migration, the transformation of D1 to S1, is not impossible. With respect to the energy obtained for D1, the more strained configuration for S1,

in-in, is endothermic by only 7 kJ/mol, while in the less strained case (configuration out-out), the process is found to be exothermic by 26 kJ/mol compared to D1. As the decomposition takes place, S1 is expected to be transformed into S2, which is found to be approximately 30 kJ/mol more stable than the original structure D1. Thus, under thermodynamic considerations, we find that the $(Si)_3N$ structure that is more likely to be present on the surface is S2. The predicted vibrational frequencies were found to be around 2095 cm^{-1} for $(Si)_2NH$ structures, and it was then concluded that a $(Si)_3N$ structure should be responsible for the continuous blueshift to 2108 cm^{-1} as the temperature increases. As indicated above, the presence of S2 can explain the two features present in the spectrum after annealing to 700 and 800 K. Therefore, the combination of our three sources of information (predicted thermodynamic values, spectroscopic evidence, and calculated vibrational data) suggests that the preferred pathway during the thermal decomposition of $(Si)NH_2$ is the subsurface pathway. Previous theoretical work proposed not only that the decomposition of $(Si)NH_2$ species is hindered kinetically but also that if such decomposition happened, the most likely mechanism for it would be the surface insertion pathway.[48,51] The next section of the discussion offers an explanation to this discrepancy.

C. Theoretical explanation for the feasibility of nitrogen insertion

The pathways for ammonia decomposition have been investigated previously by Widjaja and Musgrave,[48] Kim and Cho,[51] and Xu *et al.*[49] The more sophisticated methods used in the first two works, together with the appropriate inclusion of constraints for the atoms representing the subsurface atoms, favored the acceptance of their model, in which the $(Si)NH_2$ structures are expected to be remarkably stable and with the surface insertion more facile than the subsurface insertion pathway. On the other hand, Xu *et al.* used a smaller basis set and did not impose any constraints to their cluster models, turning them unrealistic. However, the work of Xu *et al.* gives an important clue: Backbonded insertion and subsurface migration can be more favored thermodynamically if constraints are not considered. Thus, the key for a satisfactory description of surface processes seems to be the consideration of possible ways to alleviate the tremendous strain that nitrogen insertion processes impose onto the silicon lattice. We have computationally investigated transition states involved in the formation of both surface (B1) and subsurface (S1) $(Si)_2NH$ species using the two-dimer cluster model. In our approach, one-dimer model has the decomposed $(Si)_2NH$ species, and the pathway followed corresponds to the transformation of the *neighboring* $(Si)NH_2$ into $(Si)_2NH$. As explained in Sec. I, the decomposition from $(Si)NH_2$ to $(Si)_2NH$ has an intermediate, which has a tetracoordinated N atom, $(Si)_2NH_2$. Thus, each insertion step consists of the starting and final structures, a N_{4C} intermediate, and two transition states. Figure 9 shows the four insertion mechanisms that will be studied in this section: One corresponds to the formation of the inserted structure B1 in one-dimer cluster, while the other three correspond to the

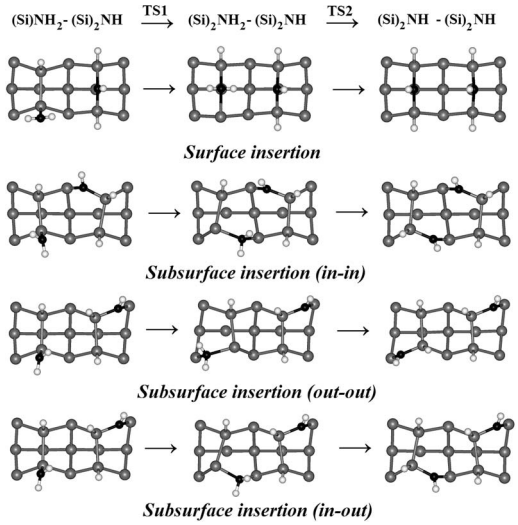

FIG. 9. Possible schemes for the nitrogen insertion mechanisms. The insertion reaction consists of an initial $(Si)NH_2$ structure, which forms the intermediate $(Si)_2NH_2$ and finally the inserted $(Si)_2NH$ structure. The neighboring structure is a bridged structure (B1) for the surface insertion scheme, while for subsurface insertion, the neighboring structure is a backbonded structure (S1) in the indicated configuration. Black, nitrogen; gray, silicon; white, hydrogen.

formation of S1 on one-dimer cluster, which can have three different configurations as discussed above. Since our approach differs from previous theoretical studies in both the way constraints are imposed to the cluster and the size of the basis sets employed, our aim is not to critically compare our data with previous results but to investigate how the energetics corresponding to subsurface insertion is affected by the configuration of the neighboring dimer. As a reference, we use the potential energy diagrams obtained from a one-dimer cluster, where subsurface atoms in the cluster were constrained in the same manner as for the larger cluster, and the same level of theory was employed.

Potential energy diagrams corresponding to the possible pathways for formation of $(Si)_2NH$ are compared in Fig. 10. Table VI compares the numerical data for these processes with the results obtained by using a one-dimer cluster. The overall barriers for the $(Si)NH_2$-$(Si)_2NH$ transformation will be further referred to as *insertion barrier*. For the surface insertion mechanism, the use of clusters representing one or two dimers does not introduce any significant difference for any of the structures, and the insertion barrier obtained is found to differ by only 3.0 kJ/mol. The differences are more pronounced for the subsurface insertion pathway, compared not only to the one-dimer case but also with respect to other configurations. When the subsurface structures are set in the out-out configuration, the stability of the structures involved is similar to the ones obtained from the one-dimer cluster model. More importantly, while the energy of the first transition state, TS1, is comparable to the other pathways, the energy to overcome the second transition state, TS2, is unusually small, and the overall insertion barrier is lowered to 227.7 kJ/mol (Table VI). For the other two subsurface configurations, the stability and the insertion barrier are found to

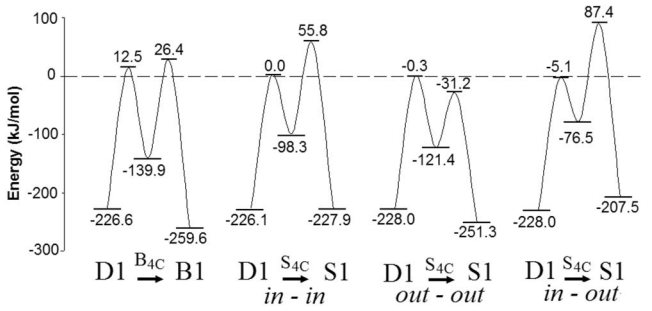

FIG. 10. Potential energy diagrams corresponding to the decomposition of $(Si)NH_2$ in presence of a neighboring $(Si)_2NH$ structure. The only possibility for surface insertion (D1→B1) and the three possibilities for subsurface insertion (S1→S2) are shown. As described in the text, each transformation consists of two transition states and a tetracoordinated intermediate (B_{4C} and S_{4C} for surface and subsurface insertions, respectively). Energy values were calculated at the B3LYP/6-31+G(*d*) level of theory and are with respect to reactant level (NH_3+empty dimer).

be higher than those for the out-out configuration. However, a closer comparison of the potential energy diagrams corresponding to in-in and in-out configurations shows an important fact: The in-in configuration produces both a N_{4C} structure and a NH backbond structure that are more stable than the in-out configuration (−98.3 vs −76.5 kJ/mol and −227.9 vs −207.5 kJ/mol, respectively). As a result, the insertion barrier is also lower for the in-in configuration (281.9 vs 315.4 kJ/mol for in-in and in-out configurations, respectively). It is worth noticing that the in-in configuration alleviates the strain almost exclusively by canceling the opposite forces imposed by the two $(Si)_2NH$ species and that further stabilization by directing the strain toward the H_{surf} entities is almost negligible. Thus, the insertion in this configuration may be a close model of the actual surface process. While the surface insertion pathway has no means to alleviate the strain imposed over the surface, we found that the first step of subsurface insertion is a process that has insertion barriers that can differ by approximately 90 kJ/mol, depending on the configuration considered. These large differences for the insertion barrier are found between processes leading to the formation of out-out and in-out configurations, despite the fact that both processes start with exactly the same structure and that the only difference is the orientation of the inserted structure. Thus, subsurface insertion should not be considered as an isolated mechanism but as a *cooperative, self-promoted process* able to originate a specific long-range configuration for inserted species. We are aware that it can be argued that the out-out configuration may not be the most realistic representation of the surface because in this case, the strain produced by the nitrogen insertion is directed toward the H_{surf} entities. However, such low barrier has not been obtained for our one-dimer calculations, not even in previous studies where an unconstrained cluster was considered.[49] The barrier observed in configuration out-out is obtained from the particular geometry of the cluster given by the orientation of the $(Si)_2NH_2$ intermediate on one-dimer cluster and a $(Si)_2NH$ intermediate on the neighboring dimer. This investigation confirms that subsurface insertion processes can be satisfactorily explained by considering that the insertion on one-dimer cluster is promoted by the structure on the neighboring dimer.

IV. SUMMARY AND FUTURE DEVELOPMENTS

The long-range configuration has been a major factor along this investigation. While for the room temperature adsorption it seems to have a tremendous influence on the spectroscopic signature observed experimentally, for the thermal decomposition, it seems to be the result of a cooperative insertion mechanism. The implications of the long-range surface arrangements to explain our results and to outline possible future applications are discussed in two separate sections.

A. Formation and decomposition of a chemisorbed layer of NH_3 on Si(100)

Since the thermodynamic stabilities of the three configurations shown in Fig. 4 are very similar to each other, any of

TABLE VI. Energetic values (kJ/mol) from the potential energy diagrams corresponding to the decomposition pathways using the two-dimer cluster as model surface. For comparison, the values using the one-dimer cluster are included. All values obtained at the B3LYP/6-31+G(*d*) level of theory. In all cases, the values are given with respect to reactants (NH_3 and the empty Si cluster). Insertion barrier refers to the overall barrier for the reaction under study.

	Two-dimer cluster				One-dimer cluster	
	Surface insertion	Subsurface insertion in-in	Subsurface insertion out-out	Subsurface insertion in-out	Surface insertion	Subsurface insertion
$(Si)NH_2$	−226.6	−226.1	−228.0	−228.0	−223.4	−223.4
TS1	12.5	0.0	−0.3	−5.1	20.6	−10.2
$(Si)_2NH_2$	−139.9	−98.3	−121.4	−76.5	−132.3	−118.7
TS2	26.4	55.8	−31.2	87.4	26.6	49.3
$(Si)_2NH$	−259.6	−227.9	−251.3	−207.5	−260.3	−249.7
Insertion barrier	253.0	281.9	227.7	315.4	250.0	272.7

these configurations could be eventually populating the surface. The predominance of a single configuration has been proposed to depend on the conditions used during the exposure of the surface, e.g., temperature, as observed by Owen *et al.*[28] The role of adsorption temperature in determining the preferential configuration is observed from the marked differences of the Si-H vibrational mode reported upon adsorption at room temperature[8,11,55] as compared to cryogenic adsorption.[23,24] Our theoretical predictions of vibrational modes using clusters representing two and three surface silicon dimers indicate that the alternate configuration will produce a signal that is redshifted with respect to the aligned configuration. We have the agglomerate configuration included in the list of possibilities, which would result from saturation of the sites available upon interdimer dissociation. No evidence of a dimer containing two NH_2 groups has been reported to date, but an STM study has found that the ammonia-saturated layer seems to show silicon dimers with the same species adsorbed on both atoms.[28] As mentioned in the previous section, at 300 K, the surface dimers are not static along a row but are constantly altering (flipping) their buckling, allowing a variety of configurations on the surface.

Decomposition of the chemisorbed layer has been followed by IR in the range 300–800 K. The unchangeable Si-H signature over the range 300–400 K indicates that $(Si)NH_2$ species are stable on the surface, suggesting the presence of a large insertion barrier that cannot be overcome at low temperatures. However, the significant transformation observed below 600 K (before desorption processes start) indicates not only that decomposed structures are thermodynamically stable but also that even though the insertion barrier may be large, it has to be below (or reasonably close to) the energy of ammonia in the gas phase and clean silicon surface, further referred to as the reactants level. In the previous section, the reluctance of $(Si)NH_2$ species toward further transformation has been attributed to strain effects. The comparison of our system to related systems, $NH_3/Si(111)$ and $PH_3/Si(100)$, can offer some insight into the effect of the strain for the system under investigation, $NH_3/Si(100)$. Adsorption of NH_3 on Si(111) at room temperature produces $(Si)NH_2$ and $(Si)_2NH$ species, and recently, an XPS study has detected both species even at 70 K.[70] Since, in essence, adsorption and decomposition are governed by very similar reactions for NH_3 on $Si(111)-7\times7$ and on $Si(100)-2\times1$, the difference in reactivity of these silicon surfaces toward the same adsorbate has been attributed to strain effects.[14,19] For a slightly different system, $PH_3/Si(100)$, computational studies have suggested that decomposed species have a significantly higher stability with respect to the chemisorbed $(Si)PH_2$ species,[67,71] and experimentally, it has been shown that at room temperature, $(Si)_2PH$ and $(Si)_3P$ species are present on the surface.[72] McDonell *et al.* has attributed the lower reactivity of NH_3 on Si(100) as compared to PH_3 to the smaller size of N with respect to P, which impedes some favorable configurations (e.g., interdimer bridges) that are possible for the $PH_3/Si(100)$ system.[71] More importantly, these authors suggest that the small size of N generates more strain in decomposed structures than in the case of P insertion. The comparison of the $NH_3/Si(100)$ system to $NH_3/Si(111)$ and $PH_3/Si(100)$ indicates that strain effects govern the behavior of $(Si)NH_2$ during thermal decomposition.

Specific identification of the decomposed species appears to be difficult. From the two possibilities considered for $(Si)_3N$ entities, and based on the low thermodynamic stability of B2, structure S2 seems to play a significant role in the decomposition. To further understand the $B1\rightarrow B2$ transformation, we evaluated the stability of the tetracoordinated intermediate involved in this reaction. Using a constrained one-dimer cluster, the stability of this N_{4C} intermediate was found to be −30.7 kJ/mol. In contrast, the N_{4C} intermediate corresponding to the reaction $S1\rightarrow S2$ has a stability of −112.5 kJ/mol, a value that is comparable to that of the N_{4C} intermediates that precede the formation of S1 and B1 (−118.7 and −132.3 kJ/mol, respectively, all of them using the same cluster model). In addition to the $(Si)_3N$ species, $(Si)_2NH$ structures (B1 and S1) cannot be ruled out based on thermodynamic considerations, and for both structures, the Si-H vibrational signature is found to be around 2095 cm^{-1}, regardless of the basis set employed, the cluster size, or long-range configuration (in the case of S1). This fact was used to suggest that the experimental signal (blueshifting to 2108 cm^{-1} at 700–800 K) has a significant contribution of $(Si)_3N$ structures. Our spectroscopic results indicate that $(Si)_2NH$ structures are never the majority of the surface species. Even at 500 K, when the decomposition has just started, the two main signals seem to correspond to $(Si)NH_2$ and $(Si)_3N$ structures. Similarly, the XPS study of Kim and Yeom found that the binding energy attributed to $(Si)_2NH$ structures is less than 10% of the overall signal at any stage of the thermal decomposition.[27] This suggests that the decomposition of $(Si)NH_2$ species occurs in two steps: first, the $(Si)NH_2\rightarrow(Si)_2NH$ step, which is expected to be rather slow because of the lattice strain produced upon insertion. Following this first initial stage, the $(Si)_2NH\rightarrow(Si)_3N$ step produces substantially more stable species. Although we did not investigate the barriers for the transformation $S1\rightarrow S2$, the theoretical work of Xu *et al.* predicts that the formation of S2 has indeed a lower kinetic requirements than the formation of S1,[49] which further supports the picture of a slow, unfavorable, first step of insertion that is followed by a faster transformation into $(Si)_3N$. This two-step model may explain the fact that previous studies reported the presence of only $(Si)NH_2$ and $(Si)_3N$ during thermal decomposition and were unable to detect $(Si)_2NH$ species.[8,13,14]

The first (slow) step of insertion, formation of $(Si)_2NH$, was studied using a two-dimer cluster. For our four models (Table VI and Fig. 10), the first kinetic barrier to overcome is close to the reactant level, suggesting that the very first step of insertion (the formation of the tetracoordinated N_{4C} intermediate) is the most energetically demanding. The magnitude of the second barrier to overcome is smaller, but since the N_{4C} intermediate produced in the first step is calculated to have the stability just slightly below the reactant level, the barrier for the second step actually surpasses the reactant level. Through the consideration of a cooperative mechanism of surface insertion, we have shown that the stability of in-

termediates and the height of kinetic barriers themselves can be lowered, and therefore, the insertion mechanism might become favorable enough to guarantee the occurrence of the reaction. We believe that our approach is more realistic than the use of a one-dimer cluster and that it might be able to explain some other cases of subsurface insertion in a way the single dimer approach cannot reach, to offer not only a kinetic description but also a thermodynamic understanding of the insertion of surface species.

Unfortunately, if, on one hand, the notion of a long-range configuration has allowed us to propose the feasibility of a subsurface insertion mechanism, on the other hand, this approach does not allow us to find energetic or vibrational values without the risk of omitting and/or misrepresenting possible configurations. It can be noted, for example, that along this study, there are no references to the subsurface insertion products resulting from aligned or agglomerate configurations, although the aligned configuration may be present in substantial concentrations. However, the consideration of the alternate model has been sufficient to demonstrate that the strain can be mitigated during nitrogen insertion. It is important, however, to mention that a requisite toward the cooperative thermal decomposition of the chemisorbed layer is the saturation of the surface. In the absence of a counterpart able to mitigate the strain imposed, an isolated $(Si)NH_2$ structure would be expected to show significant reluctance toward subsurface insertion. The picture is more complex because of the possible presence of interdimer dissociation products. Although the formation of the agglomerate configuration seems to be the result of saturation of dimers undergoing interdimer dissociation, it is likely that such possibility would be sterically hindered. If interdimer dissociation produces unsaturation of the surface, the insertion could be certainly facilitated, as predicted in the investigation of Widjaja and Musgrave.[48] However, since the maximum coverage reachable in the adsorption of ammonia on a Si(100)-2×1 surface is 0.5 monolayers[7,16,19,24] (indicating that there is a NH_3 molecule adsorbed per Si dimer), we do not expect these unoccupied Si atoms to be present on silicon surface in substantial concentration.

B. Potential applications of the NH_3-Si(100) system

The understanding of the nitridation process at the atomic level is desired in order to design strategies toward the formation of ultrathin films for the semiconductor industry. However, in addition to this application, during the past few years, a broad range of other applications has been envisioned based on the interesting properties of the ammonia interaction with silicon surface. For example, molecular electronics and surface self-assembly require understanding of not only the surface reaction mechanisms but also their control in order to manipulate the surface at a molecular level. The possibility of controlling the configuration of the adsorbed species offers other strategies for surface nanopatterning, and the control of reactions of nitrogen-containing surface species, such as lone-pair interaction with foreign molecules and hydrogen transfer, opens a possibility for applications in molecular electronics. Thus, the current research on the NH_3/Si(100) system is focused on the control of the adsorbed species and their long-range configuration.[24,28–30,40–42,45,46,70,71] It has been suggested that the preference of one configuration vs others might be influenced tremendously by the adsorption temperature.[28] In fact, the comparison of our vibrational spectra and previously reported cryogenic temperature studies (Refs. 23 and 24) shows that the preferred configuration at cryogenic temperatures is likely alternate, while at room temperature, it is aligned. It is likely that other conditions, such as pressure and time of exposure, influence the long-range configuration of adsorbates as well. Further research is necessary in order to determine the conditions necessary to selectively produce a single long-range configuration in a reaction of ammonia with a Si(100) surface. We found some evidence of this possibility in our experiments: It is apparent that the redshifted component observed in the spectrum at 300 K remains unchanged after annealing the surface to 500 K. Since the spectrum at 500 K shows that decomposition has already started, this could indicate that only one configuration is able to react. Thus, through an adequate control of the long-range configuration of adsorbed species, it could be possible to modulate the reactivity of the surface and to control the nature of the surface species. The possibility of cooperation (self-promotion) during insertion processes increases the list of handles that can be used to control surface processes, because the long-range configuration of decomposed species (and therefore a pattern) can be expected. As the surface processes are understood and a single configuration can be selectively produced, the envisioned applications of this interesting system will start to expand.

V. CONCLUSIONS

The mechanism of thermal decomposition of NH_3 on Si(100) was investigated using a combination of vibrational spectroscopy and computational methods. The highly informative Si-H stretching region of the spectra provides an important and promising signature for understanding decomposition reactions on the Si(100) surface. The formation of a saturated layer of ammonia adsorbed at room temperature produces a vibrational signature that is dependent on the long-range configuration of adsorbates. Evidence of insertion mechanisms is found at temperatures as low as 500 K, and due to the similarities between the predicted frequencies of the two proposed $(Si)_2NH$ structures (bridged and back-bonded), neither of them can be ruled out. However, the possible products of further decomposition of B1 seem to be absent from the surface based on spectroscopic and thermodynamic predictions of such products. Structures of the type of S2, on the other hand, seem to be the major component of the signal at 700 K and above, and the continuous blueshift of the Si-H vibrational mode indicates that there is indeed a $(Si)_3N$ structure present on the surface. The absence of a dominant signal around 2095 cm^{-1} suggests that $(Si)_2NH$ structures do not constitute the majority of surface species at any stage of decomposition. Our theoretical study of the decomposition pathways shows that subsurface insertion

mechanisms can be facilitated by considering configurations able to alleviate the strain imposed by the insertion process. A cooperative mechanism of insertion seems to be the explanation for the thermal decomposition of the ammonia-saturated Si(100) surface.

Note added in proof. It was pointed out in this paper that evidence of an agglomerate configuration can be obtained from the STM data of Owen *et al.* (Ref. 28). In a recent publication, these authors consider multiple ammonia dissociation pathways and note that cluster calculations do not normally consider strain effects during N insertion,[75] which is one of the goals of the present investigation.

ACKNOWLEDGMENTS

Olga Dmitrenko (Department of Chemistry and Biochemistry, University of Delaware) is acknowledged for useful discussion and suggestions. GridChem (http://www.gridchem.org)[73,74] is acknowledged for computational resources and services for the selected results used in this publication. In particular, J.C.F.R.-R. would like to thank Sudhakar Pamidighantam (National Center for Supercomputing Applications, NCSA) and Stelios Kyriacou (Ohio Supercomputer Center, OSC) for their helpful assistance during the use of GRIDCHEM. This work was supported by the National Science Foundation (CHE-0313803).

*Corresponding author; andrewt@udel.edu

[1] F. Bozso and P. Avouris, Phys. Rev. Lett. **57**, 1185 (1986).
[2] P. Avouris, F. Bozso, and R. J. Hamers, J. Vac. Sci. Technol. B **5**, 1387 (1987).
[3] E. K. Hlil, L. Kubler, J. L. Bischoff, and D. Bolmont, Phys. Rev. B **35**, 5913 (1987).
[4] R. J. Hamers, P. Avouris, and F. Bozso, Phys. Rev. Lett. **59**, 2071 (1987).
[5] R. J. Hamers, P. Avouris, and F. Bozso, J. Vac. Sci. Technol. A **6**, 508 (1988).
[6] F. Bozso and P. Avouris, Phys. Rev. B **38**, 3937 (1988).
[7] M. J. Dresser, P. A. Taylor, R. M. Wallace, W. J. Choyke, and J. J. T. Yates, Surf. Sci. **218**, 75 (1989).
[8] M. Fujisawa, Y. Taguchi, Y. Kuwahara, M. Onchi, and M. Nishijima, Phys. Rev. B **39**, 12918 (1989).
[9] P. A. Taylor, R. M. Wallace, W. J. Choyke, M. J. Dresser, and M. J. Yates, Jr., Surf. Sci. **215**, L286 (1989).
[10] J. L. Bischoff, F. Lutz, D. Bolmont, and L. Kubler, Surf. Sci. **251-252**, 170 (1991).
[11] C. U. S. Larsson and A. S. Flodstrom, Surf. Sci. **241**, 353 (1991).
[12] C. U. S. Larsson, C. B. M. Andersson, N. P. Prince, and A. S. Flodstrom, Surf. Sci. **271**, 349 (1992).
[13] X. L. Zhou, C. R. Flores, and J. M. White, Surf. Sci. **268**, L267 (1992).
[14] P. J. Chen, M. L. Colaianni, and M. J. Yates, Jr., Surf. Sci. **274**, L605 (1992).
[15] S. M. Cherif, J. P. Lacharme, and C. A. Sebenne, Surf. Sci. **262**, 33 (1992).
[16] G. Rangelov, J. Stober, B. Eisenhut, and T. Fauster, Phys. Rev. B **44**, 1954 (1991).
[17] J. L. Bischoff, F. Lutz, D. Bolmont, and L. Kubler, Surf. Sci. **248**, L240 (1991).
[18] J. L. Bischoff, L. Kubler, D. Bolmont, C. A. Sebenne, J. P. Lacharme, J. E. Bonnet, and K. Hricovini, Surf. Sci. **293**, 35 (1993).
[19] G. Dufour, F. Rochet, H. Roulet, and F. Sirotti, Surf. Sci. **304**, 33 (1994).
[20] J. Stober, B. Eisenhut, G. Rangelov, and T. Fauster, Surf. Sci. **321**, 111 (1994).
[21] N. Franco, J. Avila, M. E. Davila, M. C. Asensio, D. P. Woodruff, O. Schaff, V. Fernandez, K. M. Schindler, V. Fritzsche, and A. M. Bradshaw, Phys. Rev. Lett. **79**, 673 (1997).
[22] N. Franco, J. Avila, M. E. Davila, M. C. Asensio, D. P. Woodruff, O. Schaff, V. Fernandez, K. M. Schindler, and A. M. Bradshaw, J. Phys.: Condens. Matter **9**, 8419 (1997).
[23] C. Bater, M. Sanders, and J. J. H. Craig, Surf. Interface Anal. **29**, 208 (2000).
[24] K. T. Queeney, Y. J. Chabal, and K. Raghavachari, Phys. Rev. Lett. **86**, 1046 (2001).
[25] M. Z. Hossain, Y. Yamashita, K. Mukai, and J. Yoshinobu, Phys. Rev. B **68**, 235322 (2003).
[26] J. W. Kim, H. W. Yeom, K. J. Kong, B. D. Yu, D. Y. Ahn, Y. D. Chung, C. N. Whang, H. Yi, Y. H. Ha, and D. W. Moon, Phys. Rev. Lett. **90**, 106101 (2003).
[27] J. W. Kim and H. W. Yeom, Surf. Sci. **546**, L820 (2003).
[28] J. H. G. Owen, D. R. Bowler, S. Kusano, and K. Miki, Phys. Rev. B **72**, 113304 (2005).
[29] O. N. Chung, H. Kim, S. Chung, and J.-Y. Koo, Phys. Rev. B **73**, 033303 (2006).
[30] O. N. Chung, H. Kim, J.-Y. Koo, and S. Chung, Phys. Rev. B **74**, 193312 (2006).
[31] E. Fattal, M. R. Radeke, G. Reynolds, and E. A. Carter, J. Phys. Chem. B **101**, 8658 (1997).
[32] S. H. Lee and M. H. Kang, Phys. Rev. B **58**, 4903 (1998).
[33] Z. Loh and H. C. Kang, J. Chem. Phys. **112**, 2444 (2000).
[34] Y. Widjaja and C. B. Musgrave, Surf. Sci. **469**, 9 (2000).
[35] X. Xu, S. Kang, and T. Yamabe, Bull. Chem. Soc. Jpn. **74**, 817 (2001).
[36] R.-H. Zhou, P.-L. Cao, and S.-B. Fu, Surf. Sci. **249**, 129 (1991).
[37] N. W. Moriarty and P. V. Smith, Surf. Sci. **265**, 168 (1992).
[38] R. Miotto, G. P. Srivastava, and A. C. Ferraz, Phys. Rev. B **58**, 7944 (1998).
[39] J.-H. Cho and K. S. Kim, Phys. Rev. B **62**, 1607 (2000).
[40] G. M. Rignanese and A. Pasquarello, Surf. Sci. **490**, L614 (2001).
[41] Z. K. Smedarchina and M. Z. Zgierski, Int. J. Mol. Sci. **4**, 445 (2003).
[42] M. Z. Zgierski and Z. K. Smedarchina, Europhys. Lett. **63**, 556 (2003).
[43] J.-Y. Lee and J.-H. Cho, J. Phys. Chem. B **110**, 18455 (2006).
[44] Y. Jung, Y. Shao, M. S. Gordon, D. J. Doren, and M. Head-Gordon, J. Chem. Phys. **119**, 10917 (2003).
[45] Y. Widjaja and C. B. Musgrave, J. Chem. Phys. **120**, 1555 (2004).
[46] Y. Wang and G. S. Hwang, J. Chem. Phys. **122**, 164706 (2005).

[47] E. S. Slaughter and J. L. Gland, J. Vac. Sci. Technol. A **10**, 66 (1991).
[48] Y. Widjaja and C. B. Musgrave, Phys. Rev. B **64**, 205303 (2001).
[49] X. Xu, S. Y. Kang, and T. Yamabe, Phys. Rev. Lett. **88**, 076106 (2002).
[50] G. M. Rignanese and A. Pasquarello, Appl. Phys. Lett. **76**, 553 (2000).
[51] H.-J. Kim and J.-H. Cho, Phys. Rev. B **69**, 233402 (2004).
[52] A. L. Gerrard, J. Chen, and J. F. Weaver, J. Phys. Chem. B **109**, 8017 (2005).
[53] S. Ishidzuka, Y. Igari, T. Takaoka, and I. Kusunoki, Appl. Surf. Sci. **130-132**, 107 (1998).
[54] L. Kubler, J. L. Bischoff, and D. Bolmont, Phys. Rev. B **38**, 13113 (1988).
[55] A. C. Dillon, P. Gupta, M. B. Robinson, A. S. Bracker, and S. M. George, J. Vac. Sci. Technol. A **9**, 2222 (1991).
[56] H. Goto, K. Shibahara, and S. Yokoyama, Appl. Phys. Lett. **68**, 3257 (1996).
[57] C. Mui, Y. Widjaja, J. K. Kang, and C. B. Musgrave, Surf. Sci. **557**, 159 (2004).
[58] A. A. Bagatur'yants, K. P. Novoselov, A. A. Safonov, J. V. Cole, M. Stoker, and A. A. Korkin, Surf. Sci. **486**, 213 (2001).
[59] R. A. Wolkow, Annu. Rev. Phys. Chem. **50**, 413 (1999).
[60] S. F. Bent, J. Phys. Chem. B **106**, 2830 (2002).
[61] A. D. Becke, J. Chem. Phys. **98**, 5648 (1993).
[62] C. T. Lee, W. T. Yang, and R. G. Parr, Phys. Rev. B **37**, 785 (1988).
[63] M. J. Frisch, G. W. Trucks, H. B. Schlegel, G. E. Scuseria, M. A. Robb, J. R. Cheeseman, J. A. Montgomery, Jr., T. Vreven, K. N. Kudin, J. C. Burant, J. M. Millam, S. S. Iyengar, J. Tomasi, V. Barone, B. Mennucci, M. Cossi, G. Scalmani, N. Rega, G. A. Petersson, H. Nakatsuji, M. Hada, M. Ehara, K. Toyota, R. Fukuda, J. Hasegawa, M. Ishida, T. Nakajima, Y. Honda, O. Kitao, H. Nakai, M. Klene, X. Li, J. E. Knox, H. P. Hratchian, J. B. Cross, C. Adamo, J. Jaramillo, R. Gomperts, R. E. Stratmann, O. Yazyev, A. J. Austin, R. Cammi, C. Pomelli, J. W. Ochterski, P. Y. Ayala, K. Morokuma, G. A. Voth, P. Salvador, J. J. Dannenberg, V. G. Zakrzewski, S. Dapprich, A. D. Daniels, M. C. Strain, O. Farkas, D. K. Malick, A. D. Rabuck, K. Raghavachari, J. B. Foresman, J. V. Ortiz, Q. Cui, A. G. Baboul, S. Clifford, J. Cioslowski, B. B. Stefanov, G. Liu, A. Liashenko, P. Piskorz, I. Komaromi, R. L. Martin, D. J. Fox, T. Keith, M. A. Al-Laham, C. Y. Peng, A. Nanayakkara, M. Challacombe, P. M. W. Gill, B. Johnson, W. Chen, M. W. Wong, C. Gonzalez, and J. A. Pople, GAUSSIAN 03, Revision C. 02, Gaussian, Inc., Wallingford, CT, 2004.
[64] K. M. Bulanin, A. G. Shah, D. R. Fitzgerald, D. J. Doren, and A. V. Teplyakov, J. Phys. Chem. B **106**, 7286 (2002).
[65] L. P. Mendez de Leo, L. Pirolli, and A. V. Teplyakov, J. Phys. Chem. B **110**, 14337 (2006).
[66] K. M. Bulanin, A. G. Shah, and A. V. Teplyakov, J. Chem. Phys. **115**, 7187 (2001).
[67] R. Miotto, G. P. Srivastava, R. H. Miwa, and A. C. Ferraz, J. Chem. Phys. **114**, 9549 (2001).
[68] M. D. Halls and K. Raghavachari, J. Phys. Chem. B **108**, 19388 (2004).
[69] G. M. Rignanese and A. Pasquarello, Phys. Rev. B **63**, 075307 (2001).
[70] I. K. Cho, Y. K. Kim, and H. W. Yeom, Phys. Rev. B **73**, 115328 (2006).
[71] T. L. McDonell, N. A. Marks, O. Warschkow, H. F. Wilson, P. V. Smith, and M. W. Radny, Phys. Rev. B **72**, 193307 (2005).
[72] H. F. Wilson, O. Warschkow, N. A. Marks, S. R. Schofield, N. J. Curson, P. V. Smith, M. W. Radny, D. R. McKenzie, and M. Y. Simmons, Phys. Rev. Lett. **93**, 226102 (2004).
[73] R. Dooley, K. Milfeld, K. Guiang, S. Pamidighantam, and G. Allen, J. Grid Comput. **4**, 195 (2006).
[74] K. Milfeld, C. Guiang, S. Pamidighantam, and J. Giuliani, Proceedings of the 2005 Linux Clusters: The HPC revolution, April 2005 (unpublished).
[75] D. R. Bowler and J. H. G. Owen, Phys. Rev. B **75**, 155310 (2007).